

A comparison of triazole cross-linked polymers based on poly-AMMO and GAP: Mechanical properties and curing kinetics

Hui Li,¹ FengQi Zhao,¹ QianQian Yu,² BoZhou Wang,¹ XianMing Lu¹

¹Science and Technology on Combustion and Explosion Laboratory, Xi'an Modern Chemistry Research Institute, Xi'an, Shaanxi, 710065, China

²Department of Chemical Engineering, Shaanxi Institute of Technology, Xi'an, Shaanxi, 710300, China

Correspondence to: F. Q. Zhao (E-mail: npecc@163.com)

ABSTRACT: Triazole cross-linked polymers based on poly(3-azidomethyl-3-methyl oxetane) (poly-AMMO) and glycidyl azide polymer (GAP) were prepared using bis-propargyl-1,4-cyclohexyl-dicarboxylate (BPHA) as curing agent, respectively. Swelling tests demonstrated that cross-linking densities of the resulted polymers both increased with the increase of BPHA. Triazole cross-linked polymers based on poly-AMMO showed superior tensile strength and elongation at break than those of GAP at comparable stoichiometry. The curing kinetics was also investigated by FTIR, and GAP exhibited faster reaction rate when reacted with BPHA than that of poly-AMMO. In addition, with the increase of cross-linking density, the glass transition temperature (T_g) of as-prepared polymers significantly increased, and poly-AMMO-based polymers showed stronger T_g -raising effect than GAP-based polymers. © 2016 Wiley Periodicals, Inc. *J. Appl. Polym. Sci.* **2016**, *133*, 43341.

KEYWORDS: crosslinking; kinetics; mechanical properties

Received 21 September 2015; accepted 12 December 2015

DOI: 10.1002/app.43341

INTRODUCTION

In composite solid propellant, cross-linked polymers provide a binding matrix for the oxidizer, metallic fuel, and other additives.^{1,2} It performs the role of maintaining the structure integrity and good mechanical properties to the whole propellant grains. Moreover, it also brings high energy when energetic binders are used. Cross-linked polyurethane formed by the reaction of hydroxyl-terminated polymers and isocyanates are widely used in composite solid propellants by the virtue of high abrasion, chemical resistance and excellent mechanical properties.³ However, cross-linked polyurethane binders suffer from the humidity sensitivity of curing process, leading to deterioration of the mechanical properties of propellant.^{4–6} In addition, the inherent incompatibility of isocyanates with energetic oxidizer, such as ammonium dinitramide (ADN),^{7–9} also makes a new methodology necessary for processing high energy propellants using ADN as oxidizer.

The so-called “Huisgen reaction” of azide and alkyne is a versatile tool in polymer chemistry for realizing triazole cross-linked polymers in good yield without any side reactions, which providing a new methodology for propellant curing.^{10–13} Most of the important, triazole curing system, being insensitive to moisture, results in no special precautions to inhibit the moisture of surrounding and reactants during manufacture process. In addition,

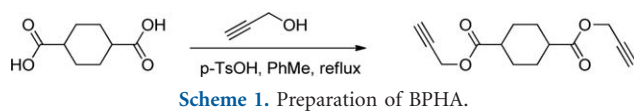
it is possible to prepare eco-friendly and smokeless propellant using ADN as oxidizer attributed to the good compatibility of ADN and triazole curing system.¹⁴ Triazole cross-linked polymers based on GAP and various alkynyl-based curing agents, including aromatic and aliphatic alkynes, were widely investigated.^{15–19} However, their mechanical properties are inferior mainly ascribed to high rigidity of GAP chain.²⁰ In poly-AMMO, the presence of more flexible backbone than GAP makes triazole cross-linked polymers based on poly-AMMO attractive.

Herein, the structure, mechanical properties and curing kinetics of triazole cross-linked polymers based on poly-AMMO were reported, which have potential applications in solid propellants. At the same time, GAP was also investigated in order to give a comparative study.

EXPERIMENTAL

Materials and Methods

Hydroxyl terminated poly-AMMO with molecular weight (M_n) of 3773 g mol⁻¹ and hydroxyl value 0.607 mmol g⁻¹ was synthesized as described in earlier study.²¹ Hydroxyl terminated GAP with molecular weight of 3623 g mol⁻¹ and hydroxyl value of 0.482 mmol g⁻¹ was purchased from Liming Research Institute of Chemical Industry (China). GAP is golden transparent

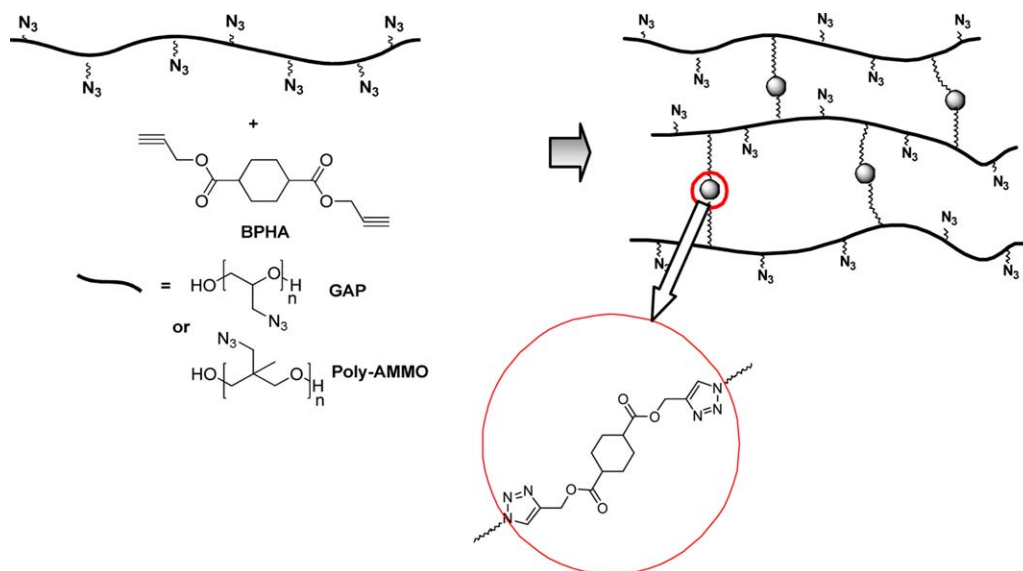


viscous liquid and poly-AMMO is colorless viscous liquid. Cyclohexane-1,4-dicarboxylic acid, propargyl alcohol and *p*-toluene sulfonic acid are analytical-grade commercial products from Energy Chemical (China).

$^1\text{H-NMR}$ and $^{13}\text{C-NMR}$ were obtained on a Bruker AV500 NMR spectrometer. Infrared spectra were obtained on a Bruker TENSOR27 Infrared spectrometer in the range of $4000\text{--}400\text{ cm}^{-1}$. Elemental analyses (C, H, and N) were performed on a VARI-EL-3 elemental analyzer. DMA was performed on a NETZSCH DMA 242C dynamic mechanical analyzer. Tensile testing was performed on INSTRON 6022 universal testing machine with a cross-head speed of 20 mm min^{-1} and a mean value of four replicates was taken. Viscosity was performed on a Brookfield CAP+ viscometer.

Synthesis of Bis-Propargyl-1,4-Cyclohexyl-Dicarboxylate (BPHA) (Scheme 1)²²

A mixture of cyclohexane-1,4-dicarboxylic acid (34.4 g, 0.2 mol), propargyl alcohol (56 g, 1 mol) and *p*-toluene sulfonic acid (1.72 g, 0.01 mol) in toluene (150 mL) was heated to reflux through a Dean-Stark apparatus for 12 h. The reaction solution was washed with 5% sodium bicarbonate solution two times with water, and dried with anhydrous sodium sulfate. Filtration and evaporation of the solvent gave white solid (32 g, 64.5%), M.p. 36.4°C . $^1\text{H-NMR}$ (DMSO- d_6 , 500 MHz): $\delta = 4.69$ (d, 4H, $J = 2.50$ Hz), 3.51 (t, 2H, $J = 2.50$ Hz), 2.56 (m, 2H), 1.71 (m, 8H); $^{13}\text{C-NMR}$ (DMSO- d_6 , 125 MHz): $\delta = 174.0, 79.0, 77.9, 52.1, 40.0, 25.8$; IR (KBr, cm^{-1}): $\nu = 3265, 2934, 2126, 1731, 1449, 1038, 996, 679$; Calc. for $\text{C}_{14}\text{H}_{16}\text{O}_4$: C 67.73, H 6.50; Found: C 67.69, H 6.52.



Scheme 2. Preparation of triazole cross-linked polymer. [Color figure can be viewed in the online issue, which is available at wileyonlinelibrary.com.]

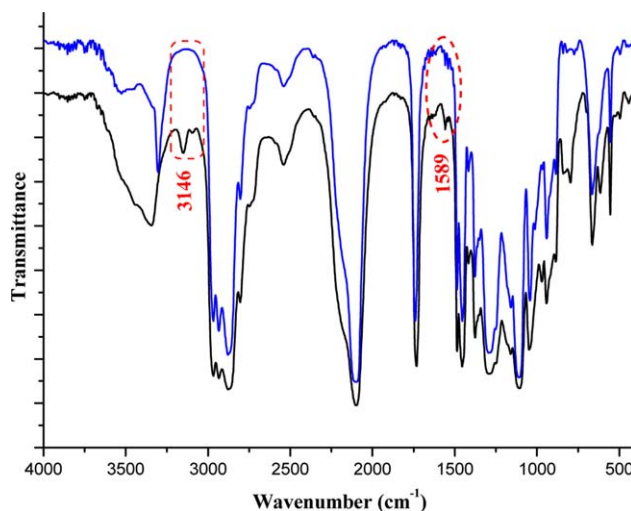


Figure 1. FTIR spectra of 1,2,3-triazole cross-linked polymers (bottom) and the blend of poly-AMMO and BPHA (above). [Color figure can be viewed in the online issue, which is available at wileyonlinelibrary.com.]

Preparation of Elastomers

In order to get similar cross-linking density as classical polyurethane network, we calculated the stoichiometric ratio of the reaction mixture with molar ratio of alkyne groups and hydroxyl end groups (R value). And the R values are 1.2, 1.4, 1.6, 1.8, and 2.0, respectively. Take Poly-AMMO-based polymer as example ($R = 1.2$), 16.086 g Poly-AMMO (0.12 mol azide) was mixed with 1.452 g of BPHA and degassed at the rotary evaporator. The clear solution (about 7 mL) was then cast into a Teflon mold and cured at 50°C for 4 days to get a clear elastomer. The preparation of triazole cross-linked polymer are shown in Scheme 2.

Swelling of Triazole Cross-Linked Polymers

The specimens were cut into similar sizes ($10\text{ mm} \times 5\text{ mm} \times 2\text{ mm}$) and immersed in solvents at room temperature for some time. Subsequently, the specimens were removed from

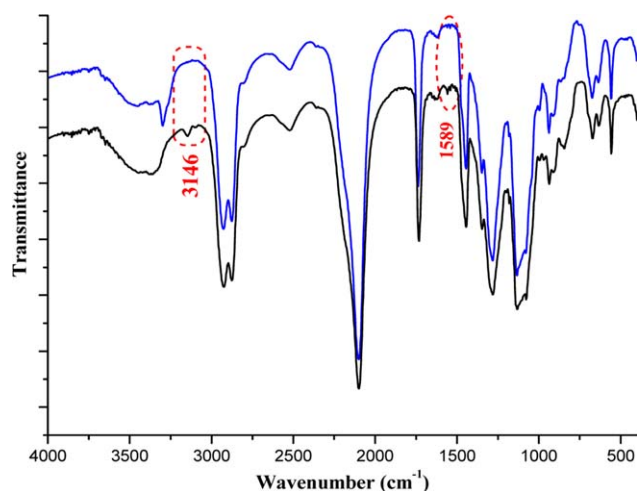


Figure 2. FTIR spectra of 1,2,3-triazole cross-linked polymers (bottom) and the blend of GAP and BPHA (above). [Color figure can be viewed in the online issue, which is available at wileyonlinelibrary.com.]

solvents, quickly blotted with dry filter paper, and weighted until the weight change were less than 0.01 g over a period of 30 min. The equilibrium swelling ratios (Q_v) were calculated using eq. (1):

$$Q_v = 1 + (w/w_0 - 1) \rho_2 / \rho_1 \quad (1)$$

Where w_0 and w are the mass of the unswollen and swollen specimens, and ρ_1 and ρ_2 are the densities of the solvent and polymer, respectively.

Kinetic Measurements. FTIR spectroscopy offers a method for evaluating the reaction rates of the curing process.^{23–25} GAP and poly-AMMO were mixed with BPHA with R value of 2, respectively. A small amount of the mixture was placed between two KBr pellets, and then placed in an oven at a given temperature. FTIR measurements were performed on a Bruker TENSOR27 Infrared spectrometer at a given time. The intensity of sp^2 C–H stretching band (3146 cm^{-1}) for triazole ring increased until the completion of the reaction, while the C=O stretching band (1733 cm^{-1}) for BPHA remained unaltered throughout the curing process. Therefore, the change of the intensity for the sp^2 C–H stretching

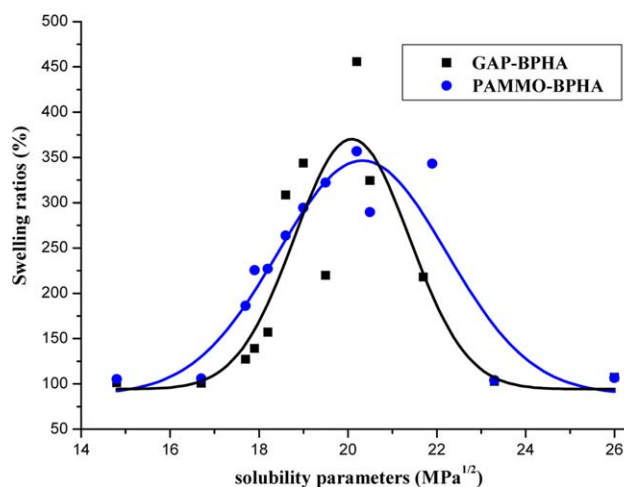


Figure 3. Equilibrium swelling ratios as a function of the solubility parameter of the solvent. [Color figure can be viewed in the online issue, which is available at wileyonlinelibrary.com.]

band relative to that of the C=O stretching band was used to evaluate the reaction rates between azide and alkyne, to ensure the results are independent to the thickness of the sample. In each case, the conversion of curing reaction, referred to as α throughout the entire study, is calculated using eq. (2):

$$\alpha = \frac{[AC-H]_t / [AC=O]_t}{[AC-H]_{ultimate} / [AC=O]_{ultimate}} \quad (2)$$

RESULTS AND DISCUSSION

Structural Characterization of 1,2,3-Triazole Cross-Linked Polymers

The predominant character of the reaction product is the formation of triazole structure. As a result, the FTIR was used to investigate the structural changes after the curing reaction. The formation of the 1,2,3-triazole cross-linked polymers-based poly-AMMO and GAP was confirmed, respectively. As shown in Figures 1 and 2, the disappearance of alkyne (3303 cm^{-1}) indicates the completion of 1,3-dipolar cycloaddition reaction. The excess of azide showed signal at 2098 cm^{-1} . In addition, the signals of triazole ring were also observed at 3146 and

Table I. Structural Parameters of Poly-AMMO and GAP-based 1,2,3-Triazole Cross-Linked Polymers

	R	ρ_2	Q_v	χ_1	v_{2m}	V	M_c (g mol ⁻¹)	N_0 (mmol cm ⁻³)
Poly-AMMO-based polymers	1.2	1.169	4.111	0.341	0.243	87	3345.1	0.349
	1.4	1.172	3.684	0.341	0.271	87	2596.4	0.451
	1.6	1.177	3.290	0.341	0.304	87	1983.7	0.593
	1.8	1.174	3.062	0.341	0.327	87	1655.8	0.709
	2	1.18	2.821	0.341	0.356	87	1349.5	0.874
GAP-based polymers	1.2	1.278	4.561	0.346	0.219	87	4719.8	0.271
	1.4	1.281	3.879	0.346	0.258	87	3261.0	0.393
	1.6	1.283	3.642	0.346	0.275	87	2812.2	0.456
	1.8	1.283	3.382	0.346	0.296	87	2352.2	0.545
	2.0	1.285	3.132	0.346	0.319	87	1948.6	0.659

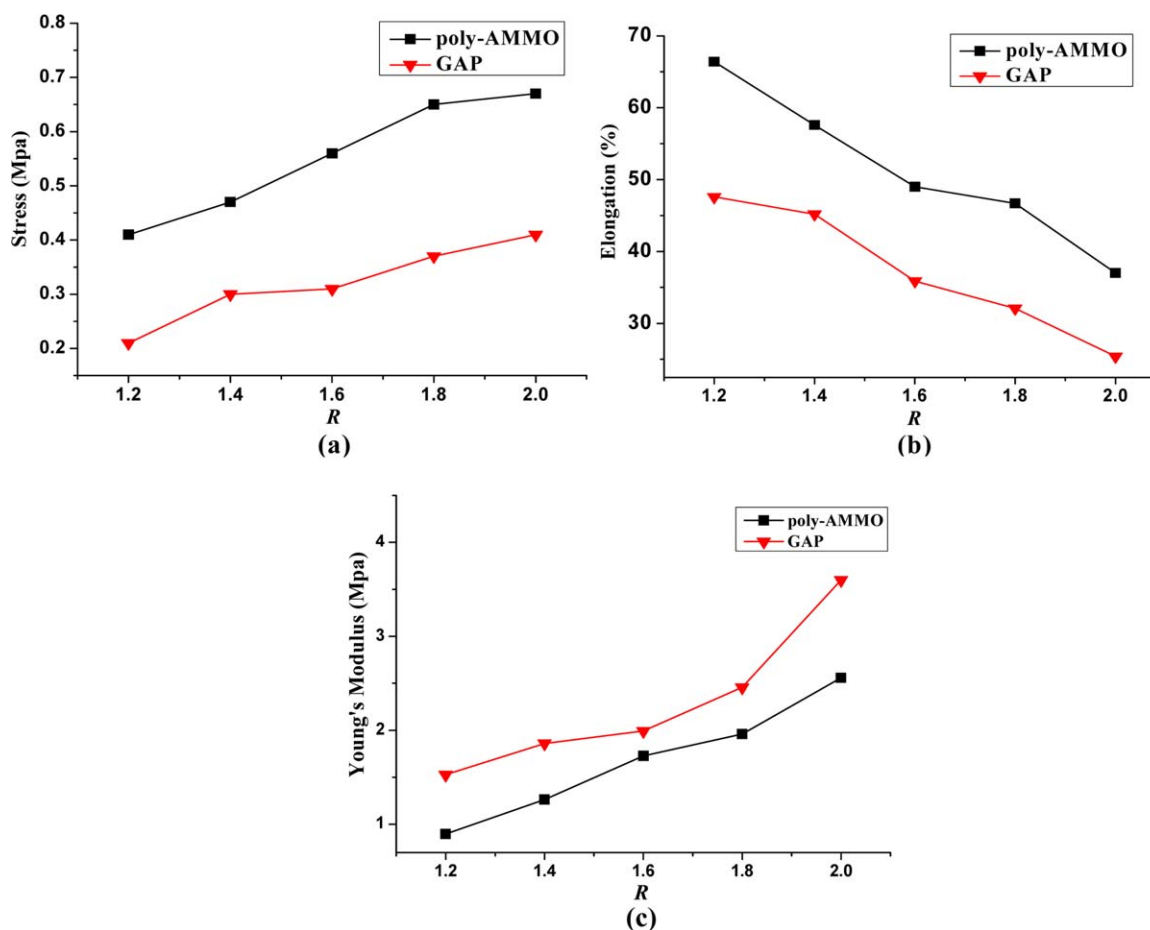


Figure 4. (a) Effect of R on the tensile strengths, (b) Effect of R on the elongation at break, (c) Effect of R on the Young's Modulus (A mean value of four replicates was taken). [Color figure can be viewed in the online issue, which is available at wileyonlinelibrary.com.]

1589 cm^{-1} , and the triazole ring as the linkage in the cross-linked polymers was confirmed. The absorption intensities of triazole ring were rather weak because of the low weight percentage of triazole ring in the resulted polymers. The other signals were similar with the blend, indicating no side reaction occurred.

Swelling Behavior

In order to obtain the solubility parameter of the 1,2,3-triazole cross-linked polymers, the polymers were swollen in various solvent with solubility parameter ranged from 14.8 to 26.0 $\text{MPa}^{1/2}$. Equilibrium swelling ratios as a function of the solubility parameter of the solvent were shown in Figure 3. Similar with

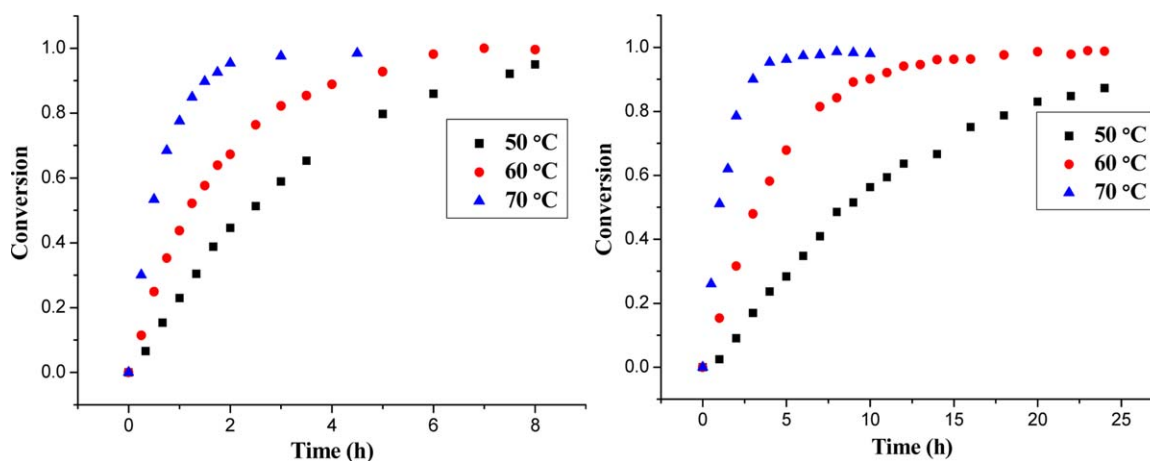


Figure 5. Kinetic curves of conversion versus time for GAP (left) and poly-AMMO when react with BPHA. [Color figure can be viewed in the online issue, which is available at wileyonlinelibrary.com.]

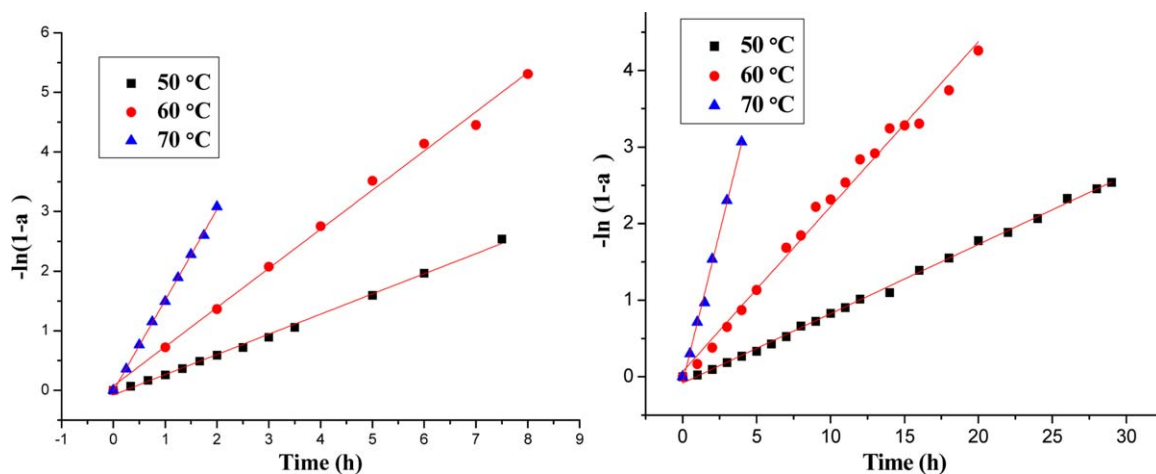


Figure 6. First-order linearization plots for GAP-BPHA (left) and poly-AMMO-BPHA (right). [Color figure can be viewed in the online issue, which is available at wileyonlinelibrary.com.]

other cross-linked polymers, Gaussian distributions can be observed in the correlation between the swelling ratio and the solubility parameter of the solvent. The solubility parameter of the polymer was determined as the solubility parameter of solvent with the maximum swelling ratio, and the solubility parameters were 20.31 and 20.09 MPa^{1/2}, for poly-AMMO and GAP-based polymers, respectively.

Based on the equilibrium swelling ratios of polymers, the volume fractions can be calculated using eq. (3). The Flory-Huggins interaction parameter between the polymer and the solvent (χ_1) can also be evaluated by the Bristow Watson Equation, eq. (4).²⁶ Thus, the average molecular weights (M_c) between the cross-linking points can be further calculated according to the Flory-Huggins theory [eq. (5)].²⁷ Meanwhile, the cross-linking densities (N_0) can also be determined, using eq. (6).

$$v_{2m} = 1/Q_v \quad (3)$$

$$\chi_1 = 0.34 + V(\delta_s - \delta_p)^2/RT \quad (4)$$

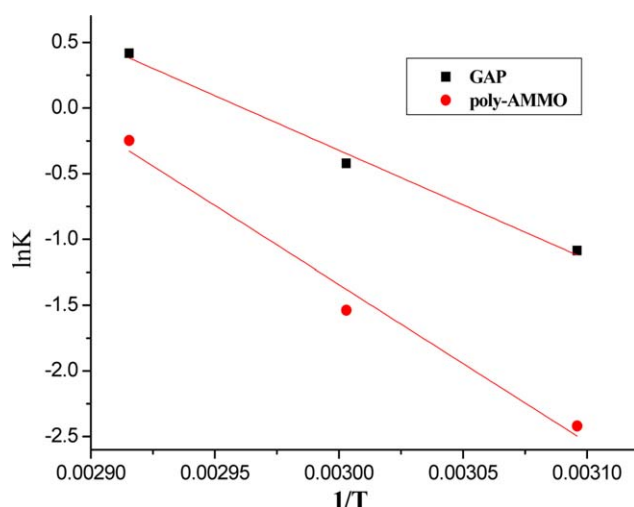


Figure 7. Arrhenius plots of the determined rate constants for GAP and poly-AMMO. [Color figure can be viewed in the online issue, which is available at wileyonlinelibrary.com.]

$$M_c = -V\rho(v_{2m}^{1/3} - v_{2m}/2)/[\ln(1 - v_{2m}) + v_{2m} + \chi_1 v_{2m}^2] \quad (5)$$

$$N_0 = \rho/M_c \quad (6)$$

Where V is the molar volume of 1, 4-dioxane (87 mL mol⁻¹), ρ is the density of the polymer. δ_p and δ_s are the solubility parameter of the polymer and the solvent, respectively. The calculated structural parameters of poly-AMMO and GAP-based polymers are listed in Table I. In fact, the amounts of azide group are far more than alkyne group. With the increase of R , N_0 increases while M_c decreases as expected. For poly-AMMO-based polymers, N_0 increases from 0.349 to 0.874 mmol cm⁻³ while M_c decreases from 3345.1 to 1349.5 g mol⁻¹. For GAP-based polymers, N_0 increases from 0.271 to 0.659 mmol cm⁻³ while M_c decreases from 4719.8 to 1948.6 g mol⁻¹. The greater cross-linking densities for poly-AMMO-based polymers at equivalent R values were attributed to the higher hydroxyl value of poly-AMMO. Moreover, the cross-linking densities of GAP-based polymers were compared with the polyurethane elastomers based on ethylene oxide-tetrahydrofuran copolymer,³ which has similar hydroxyl value with GAP used in our work. It can be found that GAP-based polymers have similar cross-linking densities with classical polyurethane network at equivalent R values.

Table II. Kinetic Parameters of Curing Reaction for GAP and Poly-AMMO with BPHA

Sample	R^2	E_a^a /kJ mol ⁻¹	A^b /s ⁻¹	Curing kinetics equation
GAP	0.992	69.2	5.0×10^{10}	$d\alpha/dt = 5.0 \times 10^{10} \exp(-8323.3/T)(1-\alpha)$
poly-AMMO	0.984	99.9	1.1×10^{15}	$d\alpha/dt = 1.1 \times 10^{15} \exp(-12.15.9/T)(1-\alpha)$

^a activation energy.

^b Pre-exponential factor.

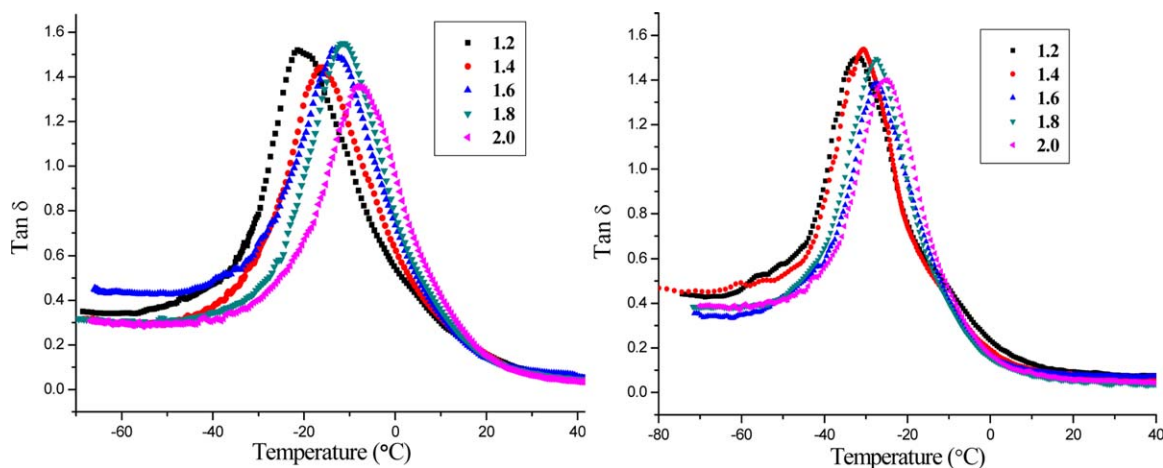


Figure 8. DMA spectra of poly-AMMO-BPHA (left) and GAP-BPHA (right) elastomer. [Color figure can be viewed in the online issue, which is available at wileyonlinelibrary.com.]

Mechanical Properties

The tensile strength, Young's modulus and elongation at break for poly-AMMO-based polymers were compared with those of GAP-based polymers. With the increasing of R , the cross-linking densities increased as expected, which lead to the increase of stiffness and tensile strength. The tensile strength of poly-AMMO and GAP-based polymers increased from 0.41 to 0.67 MPa and from 0.21 to 0.41 MPa, respectively. The Young's modulus of poly-AMMO and GAP-based polymers increased from 0.89 to 2.56 MPa and from 1.52 to 3.60 MPa, respectively. The curves of elongation at break showed the inverse tendency with the tensile strength and Young's modulus for poly-AMMO and GAP-based polymers, and the elongation at break decreased from 66.4% to 37.0% and from 47.6% to 25.4%, respectively. It can be seen from Figure 4, the tensile strength and elongation at break for poly-AMMO-based polymers were superior to those of GAP-based polymers while the Young's modulus for poly-AMMO-based polymers were inferior to those of GAP-based polymers.

It is well known that the impendent $-\text{CH}_2\text{N}_3$ inhibit the free rotation of individual main chain segments, which results in the reduction of chain flexibility.²⁸ Actually, the hindrance to rotation offered by $-\text{CH}_2\text{N}_3$ in GAP is greater than poly-AMMO because the weight percentage of $-\text{CH}_2\text{N}_3$ in GAP is higher than that of poly-AMMO. The poly-AMMO has more flexible backbone than GAP as expected. From the kinetic theory of rubber elasticity it is known that both stress and strain capability scale with chain flexibility to the one-half power.²⁹ As the result, the tensile strength and elongation at break for poly-AMMO-based polymers were superior to those of GAP-based polymers. Considering the higher rigidity of GAP chain, it is no surprise that GAP-based polymers showed higher Young's modulus. The Young's modulus of polyurethane thermoplastic elastomers

using poly-AMMO and GAP as soft segment were investigated by molecular dynamics simulation method.³⁰ And the results showed lower Young's modulus for the poly-AMMO-based thermoplastic elastomers, which is consistent with our results.

Curing Kinetics

The relationship between the conversion and time for GAP and poly-AMMO when react with BPHA at different temperature are shown in Figure 5, indicating the dependence of reaction rates on temperature. The initial slope of the curves is steeper, and gets smaller after a certain amount of time. Moreover, the conversion-time plots have a good fit to the first-order kinetic model for each temperature up to 90% of conversion (Figure 6),³¹ which allows the determination of the overall rate constants k for each temperature. Arrhenius' plot (Figure 7) of these data provides an estimation of the activation energy of curing reaction for GAP and poly-AMMO, that are 69.2 and 99.2 kJ mol^{-1} , respectively. The kinetic triplets are listed in Table II.

It can be concluded that the reaction rates of GAP are much faster than poly-AMMO at the same temperature. The substituent effects in 1, 3-dipolar cycloadditions of azides with alkynes have been investigated by the high-accuracy CBS-QB3 method.³² The results showed that substitution of azide with different substituents has a negligible effect on activation barriers. Actually, the viscosity of polymer plays an important role in the curing reaction. Higher viscosity commonly contributes to lower reaction rate because of the inhibition of molecule motion. The viscosity of poly-AMMO and GAP are measured as 5.32 and 1.80 $\text{Pa} \cdot \text{s}$ for 50°C, respectively. As a result, we conclude that the significant difference of reaction rate for poly-AMMO and GAP mainly attribute to the significant difference of viscosity.

Table III. The T_g Values for Poly-AMMO and GAP-Based Polymers

Sample	Poly-AMMO based polymers					GAP based polymers				
	1.2	1.4	1.6	1.8	2.0	1.2	1.4	1.6	1.8	2.0
T_g (°C)	-21.7	-16.3	-13.3	-11.2	-7.3	-32.3	-30.9	-28.2	-27.4	-25.1

Thermal Properties

In comparison with DSC, DMA is more sensitive and effective to determine the T_g . The dependence of loss factor on temperature for poly-AMMO and GAP-based polymers are shown in Figure 8, and the T_g values are listed in Table III. Compared with GAP-based polymers, poly-AMMO-based polymers have a stronger T_g -raising effect. With the increase of R, the T_g values for poly-AMMO and GAP-based polymers gradually increase from -21.6°C to -7.5°C and from -32.3°C to -24.6°C , respectively. In fact, the increases of cross-linking densities often shorten the distance among the cross-linking points, which contribute to the inhibition of the segment motion in poly-AMMO and GAP.

CONCLUSIONS

Bis-propargyl-1,4-cyclohexyl-dicarboxylate (BPHA) was synthesized as a new curing agent to generate triazole cross-linked polymers based on poly-AMMO and GAP, respectively. The formation of triazole cross-links was confirmed by the emergence of the triazole signals in IR. The mechanical performance of the resulted polymers can be regulated by the molar ratio of alkyne groups and hydroxyl groups. In comparison with GAP-based polymers, the poly-AMMO-based polymers showed higher stress and strain attributed to higher flexibility in poly-AMMO chain. The curing kinetics of poly-AMMO and GAP using BPHA as curing agent was carried out in the bulk state by FTIR, respectively. The conversion-time plots have a good fit to the first-order kinetic model for each temperature up to 90% of conversion, and the activation energy of curing reaction were calculated as 69.2 and 99.2 kJ mol^{-1} , respectively. Triazole cross-linked polymers based on poly-AMMO showed great potential in solid propellant by virtue of their predominant advantages of moisture insensitivity and regulated mechanical performances.

ACKNOWLEDGMENTS

This work was supported by the National Natural Science Foundation of China (21173163).

REFERENCES

1. Davenas, A. J. *Propul. Power* **2003**, *19*, 1108.
2. Reshmi, S.; Arunan, E.; Reghunadhan Nair, C. P. *Ind. Eng. Chem. Res.* **2014**, *53*, 16612.
3. Qu, Z. Y.; Zhai, J. X.; Yang, R. *J. Polym. Adv. Technol.* **2014**, *25*, 314.
4. Katritzky, A. R.; Meher, N. K.; Hancl, S.; Cyanda, R.; Tala, S. R.; Mathai, S.; Duran, R. S.; Bernard, S.; Sabri, F.; Singh, S. K.; Doskocz, J.; Ciaramitaro, D. A. *J. Polym. Sci., Part A: Polym. Chem.* **2008**, *46*, 238.
5. Manzara, A. P.; Elmo, L. M. U.S. Patent US 5681904 (1997).
6. Lee, D. H.; Kim, K. T.; Jung, H.; Kim, S. H.; Park, S.; Jeon, H. B.; Paik, H. J.; Min, B. S.; Kim, W. J. *Taiwan Inst. Chem. Eng.* **2014**, *45*, 3110.
7. Keicher, T.; Kuglstatte, W.; Eisele, S.; Wetzel, T.; Krause, H. *Propell. Explos. Pyrotech.* **2009**, *34*, 210.
8. Menke, K.; Heintz, T.; Schweikert, W.; Keicher, T.; Krause, H. *Propell. Explos. Pyrotech.* **2009**, *34*, 218.
9. Lee, D. H.; Kim, K. T.; Jang, Y.; Lee, S.; Jeon, H. B.; Paik, H. J.; Min, B. S.; Kim, W. J. *Appl. Polym. Sci.* **2014**, *131*, 40594.
10. Binder, W. H.; Sachsenhofer, R. *Macromol. Rapid Commun.* **2007**, *28*, 15.
11. Johnson, J. A.; Finn, M. G.; Koberstein, J. T.; Turro, N. S. *Macromol. Rapid Commun.* **2008**, *29*, 1052.
12. Malkoch, M.; Vestberg, R.; Gupta, N.; Mespouille, L.; Dubois, P.; Mason, A. F.; Hedrick, J. L.; Liao, Q.; Frank, C. W.; Kingsbury, K.; Hawker, C. J. *Chem. Commun.* **2006**, 2774.
13. Musa, O. M.; Sridhar, L. M.; Yuan-Huffman, Q. W. US Patent US 2010/0121022A1 (2010).
14. Pontius, H.; Bohn, M. A.; Aniol, J. 39th Int. Annual Conference of ICT, Karlsruhe, Germany, June 24-27, **2008**, S.129.1-129.34.
15. Keicher, T.; Kuglstatte, W.; Eisele, S.; Wetzel, T.; Kaiser, M.; Krause, H. 41st Int. Annual Conference of ICT, Karlsruhe, Germany, June 29-July 2, **2010**, S.12.1-12.15.
16. Ding, Y. Z.; Hu, C.; Guo, X.; Che, Y.; Huang, J. *J. Appl. Polym. Sci.* **2014**, *131*, 40007.
17. Hu, C.; Guo, X.; Jing, Y. H.; Chen, J.; Zhang, C.; Huang, J. *J. Appl. Polym. Sci.* **2014**, *131*, 40636.
18. Min, B. S.; Park, Y. C.; Yoo, J. C. *Propell. Explos. Pyrotech.* **2012**, *37*, 59.
19. Reshmi, S. K.; Vijayalakshmi, K. P.; Thomas, D.; Arunan, E.; Reghunadhan Nair, C. P. *Propell. Explos. Pyrotech.* **2013**, *38*, 525.
20. Pisharath, S.; Ang, H. G. *Polym. Degrad. Stab.* **2007**, *92*, 1365.
21. Li, N.; Gan, X. X.; Xing, Y. *Chin. J. Energ. Mater.* **2007**, *15*, 53.
22. Wotiz, J. H. Mentor and Ohio U.S. Patent US 2979538 (1961).
23. Xu, L.; Li, C.; Simon Ng, K. Y. *J. Phys. Chem. A* **2000**, *104*, 3952.
24. Bartolomeo, P.; Chailan, J. F.; Vernet, J. L. *Eur. Polym. J.* **2001**, *37*, 659.
25. Han, J. L.; Yu, C. H.; Lin, Y. H.; Hsieh, K. H. *J. Appl. Polym. Sci.* **2008**, *107*, 3891.
26. Bristowan, G. M.; Watson, D. W. F. *Trans. Faraday Soc.* **1958**, *54*, 1742.
27. Flory, P. J.; Rehner, J. *J. Chem. Phys.* **1943**, *11*, 521.
28. Stater, R. G.; Husband, D. M. *Propell. Explos. Pyrotech.* **1991**, *16*, 167.
29. Smith, T. L.; Frederick, J. E. *J. Appl. Phys.* **1945**, *36*, 2996.
30. Li, Q.; Yao, W. S.; Tan, H. M. *Chin. J. Explos. Propell.* **2007**, *4*, 13.
31. Binauld, S.; Boisson, F.; Hamaide, T.; Pascault, J. P.; Drockenmuller, E.; Fleury, E. *J. Polym. Sci. Part A: Polym. Chem.* **2008**, *46*, 5506.
32. Jones, G. O.; Houk, K. N. *J. Org. Chem.* **2008**, *73*, 1333.